

## **Advances in ECC Research**

**by V. C. Li**

**Synopsis:** This article reviews the recent advances in the research of Engineered Cementitious Composites (ECC), a class of microstructurally tailored fiber reinforced cementitious composites. The design basis, the processing routes, and some ECC performance characteristics in structural applications are highlighted. This article is dedicated to Professor Surendra Shah, in honor of his seminal contributions to research and education in advanced cementitious materials over the last several decades.

**Keywords:** composites; engineered cementitious composites(ECC); high performance fiber reinforced cementitious composites(HPFRC); repair; retrofit; seismic structures

ACI member Victor C. Li is a Professor of Civil and Environmental Engineering. He is a fellow of the American Society of Civil Engineers and the American Society of Mechanical Engineers. His areas of interest include infrastructure engineering, fracture mechanics, micromechanics, composite design, and material/structure interactions.

## INTRODUCTION

Fiber reinforced cementitious composites (FRC) can be classified into three groups. FRC employing low fiber volume fractions (<1 %) utilize the fibers for reducing shrinkage cracking [1]. FRC with moderate fiber volume fractions (between 1% and 2%) exhibit improved mechanical properties including modulus of rupture (MOR), fracture toughness, and impact resistance. The fibers in this class of FRC could be used as secondary reinforcement in structural members, such as in partial replacement of shear steel stirrups [2,3,4], or for crack width control in structures [5,6]. In the last decade or so, a third class of FRCs, generally labeled as high performance FRC, or simply HPFRC, has been introduced. HPFRC exhibits apparent strain-hardening behavior by employing high fiber contents. These HPFRCs include SIFCON (slurry infiltrated 5-20% of steel fibers, see, e.g. [7]), SIMCON (slurry infiltrated 6% steel fiber mat, [8]), and CRC matrix (using 5-10% finer steel fibers [9]). The tensile strain capacity of HPFRC is typically about 1.5% or less.

Recently, a new kind of fiber reinforced cementitious composite, known as Engineered Cementitious Composite (ECC) has been developed. ECC exhibits tensile strain-hardening behavior with strain capacity in the range of 3-7% [10,11], yet the fiber content is typically 2% by volume or less. The ultra-high ductility is achieved by optimizing the microstructure of the composite employing micromechanical models [10] that account for the mechanical interactions between the fiber, matrix and interface. These models provide guidance to tailoring of these three phases synergistically so that high composite performance can be achieved with only a moderate amount of fibers. ECC may be regarded as an optimized HPFRC.

The differences between ECC, FRC and common HPFRC are summarized in Table 1. Micromechanical calculations [10] tend to favor fibers with diameter  $d_f$  less than 50  $\mu\text{m}$ , in order to achieve strain-hardening with lower fiber volume fraction  $V_f$ . Hence polymeric fibers, often drawn to such diameters, are preferred over steel fibers, typically in the 150-500  $\mu\text{m}$  range. Steel fibers with lower  $d_f$  can in principle be manufactured, although the cost becomes prohibitively high [12].

This article highlights some recent advances in ECC research, including the theoretical guidelines for ECC development, the processing routes of ECC material, and some ECC performance characteristics in structural applications. A review of the fundamental mechanical properties of ECC in tension, flexure, shear and fracture can be found in [10].

## ECC MATERIAL DESIGN BASIS

The micromechanics of tensile strain-hardening for cementitious composites reinforced with randomly oriented short fibers have been extensively studied. The requirements for steady state crack propagation [13, 14] necessary for composite strain-hardening behavior, and the micromechanics of the  $\sigma$ - $\delta$  relationship [15] combine to provide guidelines for the tailoring of fiber, matrix and interface in order to attain strain-hardening with the minimum amount of fibers [10].

Steady state crack propagation means that a crack extends at constant ambient tensile stress  $\sigma_{ss}$ , while maintaining a constant crack opening  $\delta_{ss}$  (a flat crack, other than a near the crack tip region). Marshall and Cox [13] showed that this phenomenon prevails (over the typical Griffith type crack) when the condition

$$J_{tip} = \sigma_{ss} \delta_{ss} - \int_0^{\delta_{ss}} \sigma(\delta) d\delta \quad (1)$$

is satisfied. In Eqn. (1),  $J_{tip}$  approaches the matrix toughness  $K_m^2/E_m$  at small fiber content, appropriate for ECC since less than 3% fiber by volume is used. (The matrix fracture toughness  $K_m$  and Young's Modulus  $E_m$  are sensitive to the mix design, such as w/c ratio and sand content.) The right hand side of Eqn. (1) may be interpreted as the energy supplied by external work less that dissipated by the deformation of the "inelastic springs" at the crack tip process zone opening from 0 to  $\delta_{ss}$ . The inelastic springs concept is a convenient means of capturing the inelastic processes of fiber deformation/breakage and interface debonding/slippage of those fibers bridging across the crack faces in the process zone. Hence Eqn. (1) expresses the energy balance during steady state crack propagation.

Figure 1 schematically illustrates this energy balance concept on a fiber bridging stress-crack opening  $\sigma(\delta)$  relationship. The right hand side of Eqn. (1) is shown as the dark shaded area and is referred to as the complementary energy. Since the maximum value (hatched area) of this complementary energy  $J_b'$  occurs when the shaded area extends to the peak stress  $\sigma_0$  and crack opening  $\delta_0$ , it implies an upper limit on the matrix toughness as a condition for strain-hardening:

$$\frac{K_m^2}{E_m} \leq \sigma_0 \delta_0 - \int_0^{\delta_0} \sigma(\delta) d\delta \equiv J_b' \quad (2)$$

It is clear from Eqn. (2) that successful design of an ECC requires the tailoring of fiber, matrix and interface properties. Specifically, the fiber and interface properties control the shape of the  $\sigma(\delta)$  curve and are therefore the dominant factors governing  $J_b'$ . Composite design for strain-hardening requires the tailoring of the fiber/matrix interface to maximize the value of  $J_b'$ . Similarly the matrix composition must be designed so that the value of  $J_m = K_m^2/E_m$  is not excessive.

The shape of the  $\sigma(\delta)$  curve and especially the rising branch associated with  $J_b'$  shown in Figure 1 is related to a number of fiber/matrix interaction mechanisms. In the simplest case when fibers and matrix are in frictional contact only, the slope of the rising branch of the  $\sigma(\delta)$  curve, or the stiffness of the bridges, is mainly governed by the fiber content  $V_f$ , diameter  $d_f$ , length  $L_f$  and stiffness  $E_f$ , and the interface frictional bond  $\phi$ . In the case when chemical bond  $G_d$  is present, the starting point of the  $\sigma(\delta)$  is not at the origin of the plot, but is shifted upwards. This reflects the need of a certain amount of load on the fibers and interface before the interfacial chemical bond is broken. Dedonding is needed to allow for stretching of the debonded fiber segment to produce crack opening  $\delta$ . Thus the presence of  $G_d$  typically diminishes the complementary energy  $J_b'$  and is not conducive to strain-hardening. It is, however, helpful for minimizing the crack width of the multiple cracks if strain-hardening is achieved.

The peak value of the  $\sigma(\delta)$  curve is mainly governed by  $V_f$ ,  $d_f$ ,  $L_f$ ,  $\phi$  in the case of simple friction pull-out. An analytic expression of  $\sigma(\delta)$  and  $\sigma_D$  can be found in [14]. In the case when both interface chemical bond and slip-hardening are present, an analytic expression of  $\sigma(\delta)$  can be found in [16]. In the presence of  $G_d$ , the higher load on the fiber can lead to fiber rupture. Thus for given fiber strength  $\sigma_f$ , the complementary energy  $J_b'$  again decreases with  $G_d$ .

It should be emphasized that Eqn. (2) does not prescribe a particular fiber type for ECC. Rather, it is the combination of fiber, matrix and interface parameters that creates the satisfaction of the strain-hardening condition. However, there are indeed certain characteristics of fibers which enhances  $J_b'$ . These include e.g., small  $d_f$ , high  $L_f$  and low  $G_d$ . Any fiber with the correct profile of properties can in principle be a suitable fiber for ECC reinforcement.

Since  $J_b'$  increases with  $V_f$ , Eqn. (2) can be used to define a critical fiber volume fraction  $V_f^{crit}$  above which strain-hardening is expected to occur (when the inequality sign just holds), for given fiber, matrix and interface properties. Figure 2 plots  $V_f^{crit}$  as a function of interfacial friction  $\phi$  (while keeping all other micromechanical parameters fixed). For PE (polyethylene) fiber, the  $V_f^{crit}$  continues to drop with increasing  $\phi$  since the fiber strength is very high. In addition, the hydrophobic fiber does not have a chemical bond ( $G_d = 0$ ) so that fiber rupture does not usually happen. (Fiber rupture can still occur if  $L_f$  is excessively large. However, the material will not be processible.) For PVA fiber, the critical fiber volume fraction  $V_f^{crit}$  first drops but then rises again due to fiber rupture at increasingly high  $\phi$ . Fiber rupture in the hydrophilic PVA fiber is enhanced by strong chemical bonding due to the presence of the hydroxyl group in the PVA (polyvinyl alcohol) fiber, resulting in a high  $G_d$ .

The concepts expressed in Eqn. (2) for strain-hardening condition have been validated by at least two studies involving ECC composites with PE and PVA fibers. Li et al [17] studied the transition from quasi-brittle to ductile behavior for a

set of composites reinforced with PE fibers. They varied the sand content in the matrix which directly influenced the matrix toughness and the interface properties. Figure 3a shows the theoretical boundary between strain-hardening and quasi-brittle behavior using Eqn. (2) and the positions in the ( $\phi$ ,  $J_m$ ) space for the four composites tested. The tensile stress-strain responses of the four composites are shown in Figure 3b. It is clear that in the region of low  $J_m$  and high  $\phi$  (with low sand content S:C = 0 - 0.5) where Eqn. (2) predicts strain-hardening, the corresponding composites (Mix I and III) revealed tensile strains of 2.27 - 5.44%. In contrast, the composite (Mix II) with high  $J_m$  (with high sand content S:C = 2) showed poor ductility of 0.20%.

A recent study by [11] demonstrated the validity and effectiveness of using Eqn. (2) for composite constituent tailoring. For a fixed fiber volume fraction ( $V_f = 2\%$ ) and matrix toughness ( $J_m = 5 \text{ J/m}^2$ ), target values of  $\phi$ ,  $G_d$  and  $\beta$  have been determined by Wu [18] as 1 - 2.1 MPa, 0 - 2.2  $\text{J/m}^2$ , and 0 - 1.5 respectively in order to satisfy the inequality sign of Eqn. (2) for strain-hardening. These values have taken into account the variability of flaw size in the matrix [19]. The interface values were found to be successively reduced by increasing the amount of oiling agent on the fiber. When these  $\phi$ ,  $G_d$  parameters approached or dropped below the target values, the ductility of the composite was greatly enhanced.

Figure 4 shows the decreasing values of  $\phi$  and  $G_d$  as a function of oiling agent measured in single fiber pull-out tests, as well as the target values determined theoretically. This set of data suggests that oiling agent in excess of 0.6-0.8% is needed to achieve strain-hardening. Composite tensile tests using the same fiber and the same five levels of oiling content reveal that the ductility was enhanced from less than 1% to more than about 5% (Figure 5). The tensile strain capacity and multiple crack spacing as a function of oil content are shown in Figure 6. It is clear that the composite reaches multiple crack saturation when the oiling content reaches about 0.6-0.8% as expected.

The above discussions reveal that the design strategies for PE-ECC and PVA-ECC are very different. For the PE fiber with very high tensile strength and low bond properties, enhancing the interface bond strength leads to strain-hardening. An attempt to increase bond strength of PE fibers using plasma treatment process was demonstrated by Li et al [20], resulting in composites with tensile strain capacity of up to 7%. In contrast, for the PVA fiber with high chemical bond and moderate fiber strength, the design strategy calls for a reduction in interfacial chemical and frictional bond. In both cases, the matrix composition must be controlled to limit the toughness. These design strategies are rooted in micromechanics which provides guidelines for tailoring of material constituents for targeted composite performance.

## ECC PROCESSING

Two types of processing routes have been developed for ECC. For casting, normal casting and self-compacting casting [21-23] are available. Extrusion of ECC has

also been demonstrated [24]. Spray ECC, equivalent to shotcreting, but replacing the concrete with ECC, is now being developed at the University of Michigan.

Figure 7a shows a PE-ECC pipe being extruded. The resulting pipe is very ductile under ring loading, as shown in Figure 7b. Instead of the typical brittle fractures at the four hinge zones, the PE-ECC pipe exhibits 'plastic' yielding type behavior. This figure also shows the typical FRC quasi-brittle behavior of a similarly extruded pipe containing 7% of pp-fiber.

Li and co-workers [21-23] developed self-compacting ECC via a constitutive rheological approach. In this approach, the ingredients of the mortar matrix were tailored so that high flowability is achieved, while respecting the conditions of strain-hardening for the composite as described earlier. The high flowability mortar matrix results from an optimal combination of a strong polyelectrolyte (a superplasticizer) and a non-ionic polymer with steric action in maintaining non-aggregation of the cement particle in the dense suspension. Figure 8 shows the result of a deformability test and box test of a self-compacting PVA-ECC. The deformability  $\Gamma$ -value and the self-compactability  $L$ -value achieved in these tests ( $\Gamma = 11.7$ ;  $L = 0.94$ ) are comparable to those acceptable ( $\Gamma = 8$  to 12;  $L = 0.73$  to 1.00) for self-compacting concrete [25]. Tensile strain-hardening of these materials was reported [22-23].

### ECC PERFORMANCE CHARACTERISTICS IN STRUCTURAL APPLICATIONS

A number of investigations into the use of ECC in enhancing structural performance have been conducted in recent years. These include the repair and retrofit of pavements or bridge decks [26-28]; the retrofit of building walls to withstand strong seismic loading [29-31]; and the design of new framing systems [32]. These studies often reveal unique characteristics of ECC and R/ECC (steel reinforced ECC) in a structural context. These include high damage tolerance, resistance to shear load, energy absorption, delamination and spall resistance, and high deformability and tight crack width control for durability. These characteristics are illustrated with highlights of experimental results below.

**Damage Tolerance:** The damage tolerance of a structure is the ability for the structure to sustain load-carrying capacity even when overloaded into the inelastic range. For civil infrastructure systems, the cost of repair after a major earthquake can be enormous, as the 1995 Kobe earthquake in Japan (U.S.\$95-147 billion [33]) demonstrated. Hence, damage tolerance of infrastructure is critical for both safety and economic reasons.

Parra-Montesinos and Wight [32] conducted a series of cyclic tests on the structural integrity of joints in hybrid steel-beam R/C column connections. Figure 9a,b shows the contrasts of the damage experienced by the standard connection and that

experienced by a connection where the joint concrete is replaced by ECC. The corresponding load - joint deformation is shown in Figure 9c,d. The standard R/C joint suffers large crack opening, loss of bond between the axial reinforcement and the concrete, and therefore composite action, and experienced severe spalling where the steel beam bears on the concrete. In contrast, the ECC joint underwent strain-hardening with multiple micro-crack damage. The R/ECC material maintained high bond efficiency and no spalling was observed. All these were accomplished despite eliminating all the shear reinforcement used in the R/C specimen. Although the load and deflection imposed were pushed to higher levels, no repair was needed in the R/ECC connection. This experiment also demonstrated that spall failure commonly observed in high stress-concentration zones when concrete and steel elements interact can be eliminated by virtue of the damage tolerance of ECC material.

**Shear Resistance:** In R/C elements, shear failures are typically resisted by shear reinforcements in the form of dowel bars, stirrups or hoop reinforcement. However, shear failures in short columns in bridge piers or walls between stories in buildings continue to be observed after large earthquakes. The intrinsic brittleness of concrete makes it difficult to prevent shear failure that reflects the diagonal tensile stresses, potentially leading to catastrophic modes of collapse.

Kanda et al [29] and Fukuyama et al [34] conducted cyclic shear experiments on beam elements. The contrast in failure modes of the R/C and R/ECC beams can be seen in Figure 10a [34]. The corresponding cyclic load-deformation curves (Figure 10b) confirm that the shear ductility of R/ECC is superior to that of R/C. For ECC, shear damage is similar to ductile tensile damage with diagonal microcracks.

**Energy Absorption:** In seismic structures, energy absorption in hinge zones is used to dissipate the earthquake energy input. In R/C structures, the concept of a plastic hinge is introduced by ductile yielding of the steel reinforcement in seismic detailing. However, it is typical that only a small fraction of the steel actually undergoes yielding due to the disintegration of the surrounding brittle concrete.

Fischer and Li [35] conducted cyclic flexural experiments on cantilevered elements. The contrast in failure modes of the R/C and R/ECC beams is shown in Figure 11a,b. The corresponding cyclic load-deformation curves (Figure 11c,d) reveal that the R/ECC absorbs much higher energy than the R/C element. This is particularly noteworthy since no hoop shear reinforcement was utilized in the R/ECC element.

**Resistance to Delamination and Spalling in Repaired Concrete Structures:** In patch repairs, the common failure modes are spalling and/or delamination between the new and old concrete. In bridge deck or pavements overlay repairs, reflective crack and spalling in the concrete overlays and/or delamination between the bonded overlay and the old concrete substrate are often observed. It appears difficult to resist all modes of failure simultaneously since strengthening the interfacial bond tends to encourage spalling while enhancing the overlay strength tends to encourage

delamination. As a result, the durability of concrete repair is compromised by one or the other of these failure mechanisms.

Li and co-workers [26-28] studied the resistance to delamination and spalling using ECC as the repair material. Using a specimen simulating an overlay on top of a joint together with an initial interface defect, they found that the delamination and spalling modes can be both eliminated by means of a kink-crack trapping process (Figure 12a). As the four point bend load increases, the initial interface crack extends slightly but quickly kink into the ECC overlay. The kink crack was subsequently trapped in the ECC so that further load increase forces crack extension into the interface. The kinking-trapping process then repeats itself, resulting in a succession of kink cracks in the ECC. However, spalling of the ECC was not observed since the kink crack does not propagate to the specimen surface. Delamination of the interface was also eliminated since the interface crack tip repeatedly kink into the ECC. In contrast, the specimen with a regular FRC overlay shows the expected kink-spall brittle fracture behavior. The corresponding load-deformation curves for the two specimens are shown in Fig. 12b.

**Deformability:** Under restrained drying shrinkage and/or temperature loading, concrete slabs may crack and undermine durability of the slab structure (e.g. bridge decks, parking garage slabs, factory floor slabs). Such problems have typically been dealt with by introducing joints. However the joints themselves often result in damage and are costly to maintain, especially in bridge decks. The large strain capacity of ECC can be utilized to accommodate imposed deformation on the deck by replacing standard joints with a strip of ECC material. This concept was test by Zhang et al [36].

Figure 13a shows a specimen containing a strip of ECC sandwiched between two standard concrete slabs shaped into a dog-bone for tensile loading, simulating restrained shrinkage. Even when the overall specimen has loaded to over 1.3% strain (Figure 13b), the concrete slabs experienced no cracks. Instead, the imposed deformation was localized into the ECC ductile strip which underwent tensile strain-hardening. Multiple microcrack damage is shown in the inset of Figure 13a.

**Durability of Concrete Cover:** In R/C beams serious durability problems may occur due to cracking of the concrete in the tensile zone, migration of aggressive agents through the concrete cover, corrosion of the reinforcing steel, expansion of the corroded steel bar, spall-fracturing of the concrete cover, subsequent accelerated corrosion of the reinforcing bar, and loss of load-carrying capacity of the R/C beam. Such durability problems are especially common in structures such as parking garages in cold regions where deicing salts are applied to the slabs. Maalej and Li [37] investigated the use of ECC as the cover material replacing standard concrete.

In four point bend tests loading to concrete crushing on the compression side, the standard R/C beam shows a large crack width which grows rapidly after steel yielding on the tension side. In contrast, the R/C beams with an ECC cover show crack width limited to 0.2 mm throughout the whole test range (Figure 14). Since

the permeability of cracked concrete has been shown to scale with the cube of the crack width, the restriction of crack width is expected to slow down the migration of aggressive agents and therefore the corrosion rate of the re-bars, resulting in enhanced durability of the R/C structure.

## CONCLUSIONS

From the above discussions, it is clear that ECC has significant advantages in material performance over concrete and standard FRC. It also has cost and processing advantages over most common HPFRC due to its relatively low fiber content. As a result, it is plausible to envision ECC being applied to new structures such as moment frames [32] and R/C structures with ECC cover [36]. Applications of ECC to structural repair in the form of patch repair or as overlays [26-28] are plausible. Self-compacting processing [21-23] and spray processing will make these repair applications even more attractive. From the energy absorption point of view, the use of ECC in seismic retrofitting in building [29] and especially in hospitals [31] may be logical directions. Many of these application possibilities will require further investigations, but the research work that has been carried out lays a sound foundation for the use of ECC in enhancing the performance of infrastructure systems.

Further materials development of ECC may be expected in the areas of adaptation to lower cost material ingredients, adaptation of material ingredients and mixing methods to achieve desirable fresh properties for various processing routes, the addition of special functionalities to the hardened material performance, and standardization of material for easy adoption by industrial concerns. For structural applications, there is a strong need for standardized testing and design guidelines. The Japanese Concrete Institute has recently formed a Committee to investigate these issues. Novel structural systems with smart responses to loading and that take advantage of the unique characteristics of ECC may be expected. A truly high performance concrete material should embody strength, ductility, durability, cost-effective and easy and flexible processing routes. ECC represents an attempt towards this ideal.

## REFERENCES

- [1] Balaguru, P., and S. Shah, *Fiber Reinforced Cement Composites*, McGraw Hill, 1992.
- [2] Batson, G., Jenkins, E. Spatney, R., "Steel fibers as shear reinforcement in beams", *ACI Journal*, 69, 10, 640-644, 1972.
- [3] Sharma, A. K., "Shear strength of steel fiber reinforced concrete beams", *ACI proceedings*, 83, 4, 624-628, 1986.
- [4] Swamy, R.N., Bahia, H.M., "The effectiveness of steel fibers as shear reinforcement", *Concrete International*, 35-40, 1985.
- [5] Stang, H., Aarre, T. "Evaluation of crack width in FRC with conventional reinforcement", *Cement & Concrete Composite*, 14, 2, 143-154, 1992.
- [6] Stang, H., Li, V.C., Krenchel, H. "Design and structural applications of stress-crack width relations in FRC", *RILEM J. Materials and Structures*, 1993.
- [7] Naaman, A.E., and Homrich, J.R., "Tensile stress-strain properties of SIFCON" *ACI Materials J.*, 86, 3, 244-251, 1989.
- [8] Krstulovic-Opara, N., and H. Toutanji, "Infrastructural repair and retrofit with HPRFRCCs," in *High Performance Fiber Reinforced Cement Composites 2*, Eds. Naaman, A.E., and H.W. Reinhardt, E&FN Spon, 423-439, 1996.
- [9] Bache, H.H., *Introduction to Compact Reinforced Composites*, Nordic Concrete Research, Publication N6, 19-33, 1987.
- [10] Li, V.C., "Engineered Cementitious Composites - Tailored Composites Through Micromechanical Modeling," in *Fiber Reinforced Concrete: Present and the Future*. Eds. N. Banthia et al, CSCE, Montreal, 64-97, 1998.
- [11] Li, V.C., S. Wang, and C. Wu, "Tensile Strain-Hardening Behavior of PVA-ECC", Submitted, *ACI J. of Materials*, Jan., 2001.
- [12] Bakaert Corp., Belgium, private communication, 2000.
- [13] Marshall, D. and Cox, B.N. "A J-integral Method for Calculating Steady-State Matrix Cracking Stress in Composites," *Mechanics of Materials* 7, 127-133, 1988.
- [14] Li, V.C., "Post-Crack Scaling Relations for Fiber Reinforced Cementitious Composites", *ASCE J. Materials in Civil Engineering*, 4(1), 41-57, 1992.
- [15] Li, V.C. and Leung, C.K.Y., Steady State And Multiple Cracking Of Short Random Fiber Composites, *ASCE J. Engineering Mech.*, 118(11) 1992, 2246-2264.
- [16] Lin, Z., T. Kanda and V.C. Li, "On Interface Property Characterization and Performance of Fiber Reinforced Cementitious Composites," *J. Concrete Science and Engineering*, *RILEM*, 1, 173-184, 1999.
- [17] Li, V.C., D.K. Mishra and H.C. Wu, "Matrix Design for Pseudo Strain-Hardening Fiber Reinforced Cementitious Composites," *RILEM J. Materials and Structures*, 28(183), 586-595, 1995.
- [18] Wu, C., "Micromechanical Tailoring of PVA-ECC for Structural Applications," PhD Thesis, Department of Civil and Environmental Engineering, University of Michigan, Ann Arbor, USA, Jan., 2001.
- [19] Kanda, T. and V.C. Li, "A New Micromechanics Design Theory for Pseudo Strain Hardening Cementitious Composite," *ASCE J. of Engineering Mechanics*, 125(4), 373-381, 1999.
- [20] Li, V.C., H.C. Wu, and Y.W. Chan, "Effect of Plasma Treatment of Polyethylene Fibers on Interface and Cementitious Composite Properties," *J. of Amer. Ceramics Soc.*, 79(3), 700-704, 1996.
- [21] Li, V.C., H.J. Kong, and Y.W. Chan, "Development of Self-Compacting Engineered Cementitious Composites," in *Proceedings, International Workshop on Self-Compacting Concrete*, Kochi, Japan, 46-59, 1998.
- [22] Li, V.C., J. Kong, and S. Bike, "High Performance Fiber Reinforced Concrete Materials," in *Proc. of High Performance Concrete - Workability, Strength, and Durability*, 71-86, Eds. C.K.Y. Leung et al, China, 2000.
- [23] Li, V.C., J. Kong, and S. Bike, "Constitutive Rheological Design For Development Of Self-Compacting Engineered Cementitious Composites", In *Proc., 2<sup>nd</sup> Int'l Workshop on Self-Compacting Concrete*, Tokyo, Japan, 2001.
- [24] Stang, H. and V.C. Li, "Extrusion of ECC-Material", in *Proc. Of High Performance Fiber Reinforced Cement Composites 3 (HPRCC 3)*, Ed. H. Reinhardt and A. Naaman, Chapman & Hull, pp. 203-212, 1999.
- [25] Ozawa, K., Sakata, N., and Okamura, H., "Evaluation of Self-Compactability of Fresh Concrete Using the Funnel Test", *J. SCE Concrete library*, 25, 59-75, 1995.
- [26] Lim, Y.M. and V.C. Li, "Durable Repair of Aged Infrastructures Using Trapping Mechanism of Engineered Cementitious Composites" *J. Cement and Concrete Composites*, 19(4) 373-385, 1997.

- [27] Kamada, T. and V.C. Li, "The Effects of Surface Preparation on the Fracture Behavior of ECC/Concrete Repair System," *J. of Cement and Concrete Composites*, 22, 6, 423-431, 2000.
- [28] Zhang, J. and V.C. Li, "Monotonic and Fatigue Performance in Bending of Fiber Reinforced Engineered Cementitious Composite in Overlay System," Accepted, *J. of Cement and Concrete Research*, 2001.
- [29] Kanda, T., S. Watanabe and V. C. Li, "Application of Pseudo Strain Hardening Cementitious Composites to Shear Resistant Structural Elements", in *Fracture Mechanics of Concrete Structures* Proc. FRAMCOS-3, AEDIFICATIO Publishers, D-79104 Freiburg, Germany, 1477-1490, 1998.
- [30] Kabele, P., V.C. Li, H. Horii, T. Kanda and S. Takeuchi, "Use of BMC for Ductile Structural Members," in Proc. of 5th Int'l Symp. on *Brittle Matrix Composites* (BMC-5), Warsaw, Poland, 579-588, 1997.
- [31] Kesner, K.E., and S. L. Billington, "Investigation of Ductile Cement-Based Composites for Seismic Strengthening and Retrofit," in *Fracture Mechanics of Concrete Structures*, de Bost et al (eds), A.A. Balkema, Netherlands, 65-72, 2001.
- [32] Parra-Montesinos, G.J., and J.K. Wight, "Seismic Response of Exterior RC Column-to-Steel Beam Connections," ASCE J. Structural Engineering, 1113-1121, 2000.
- [33] EQE International, "The January 17, 1995 Kobe Earthquake", An EQE Summary Report, April 1995.
- [34] Fukuyama, H., Y. Matsuzaki, K. Nakano, and Y. Sato, "Structural Performance of Beam Elements with PVA-ECC," in Proc. Of High Performance Fiber Reinforced Cement Composites 3 (HPFRCC 3), Ed. Reinhardt and A. Naaman, Chapman & Hull, pp. 531-542, 1999.
- [35] Fischer, G., and V.C. Li, "Influence of Matrix Ductility on the Tension-Stiffening Behavior of Steel Reinforced Engineered Cementitious Composites (ECC)," Accepted, *ACI J. of Structures*, Jan., 2001.
- [36] Zhang, J., V.C. Li, A. Nowak and S. Wang, "Introducing Ductile Strip for Durability Enhancement of Concrete Slabs," Accepted, *ASCE J. of Materials in Civil Engineering*, April, 2001.
- [37] Maalej, M., and V.C. Li, "Introduction of Strain Hardening Engineered Cementitious Composites in the Design of Reinforced Concrete Flexural Members for Improved Durability," *ACI Structural J.*, 92(2), 167-176, 1995.

Table 1: Comparison between FRC, common HPFRC and ECC

	FRC	Common HPFRC	ECC
<b>Composite Design Methodology</b>	NA	Use high $V_f$	Micromechanics based, minimize $V_f$ for cost and processability
<b>Fiber</b>	Any type, $V_f$ usually < 2%; $d_f$ (steel) ~ 500 $\mu\text{m}$	Mostly steel, $V_f$ usually > 5%; $d_f$ ~ 150 $\mu\text{m}$	Tailored, polymer fibers most suitable; $V_f$ usually < 2%; $d_f$ < 50 $\mu\text{m}$
<b>Matrix</b>	Coarse aggregates used	Fine aggregates used	Controlled for matrix toughness and initial flaw size; fine sand used
<b>Interface</b>	Not controlled	Not controlled	$G_i$ and $\tau_0$ controlled
<b>Tensile behavior</b>	Strain-softening	Strain-hardening	Strain-hardening
<b>Tensile strain capacity</b>	0.1%	< 1.5%	> 3%; 8% demonstrated
<b>Crack width</b>	Unlimited	Typically several hundred $\mu\text{m}$ , unlimited for $\epsilon > 1.5\%$	Typically < 100 $\mu\text{m}$ during strain-hardening
<b>Processing</b>	Self-compaction demonstrated; Extrudability demonstrated	Self-compaction impossible due to high $V_f$ ; often requires high frequency vibration (e.g. in CRC); Extrudability demonstrated	Self-compaction demonstrated; Extrudability demonstrated

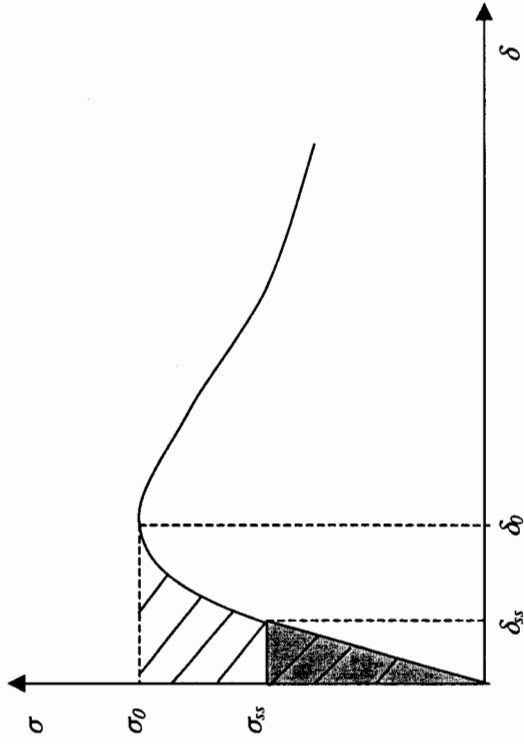
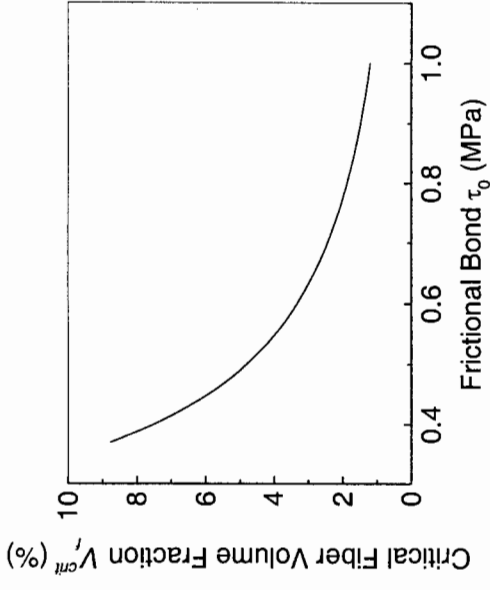


Figure 1: Schematic illustration of energy balance concept on a fiber bridging stress-crack opening  $\sigma(\delta)$  plot

(a)



(b)

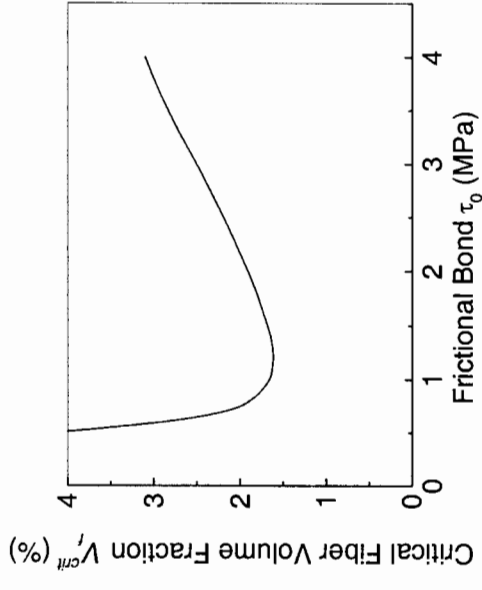


Figure 2:  $V_f^{crit}$  illustrated as a function of interfacial friction  $\tau_0$  (a) for PE-ECC; (b) for PVA-ECC. All other dependent parameters fixed.



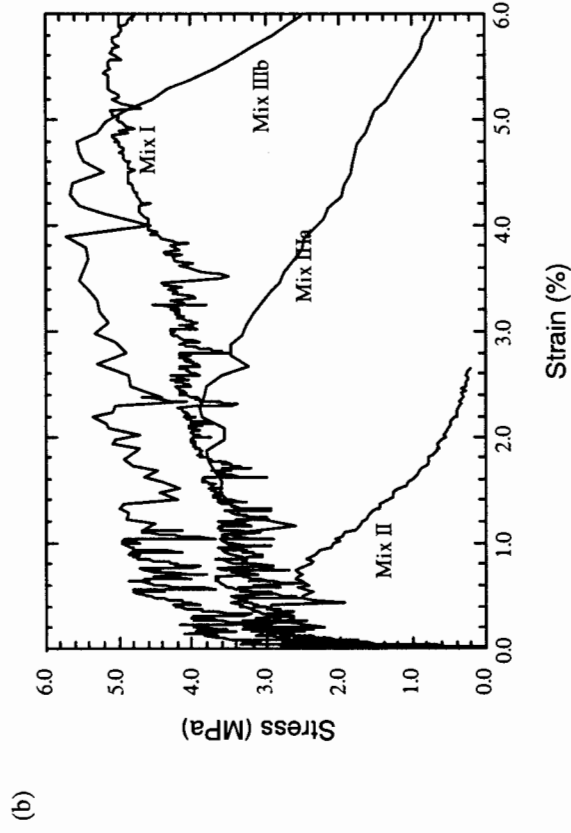
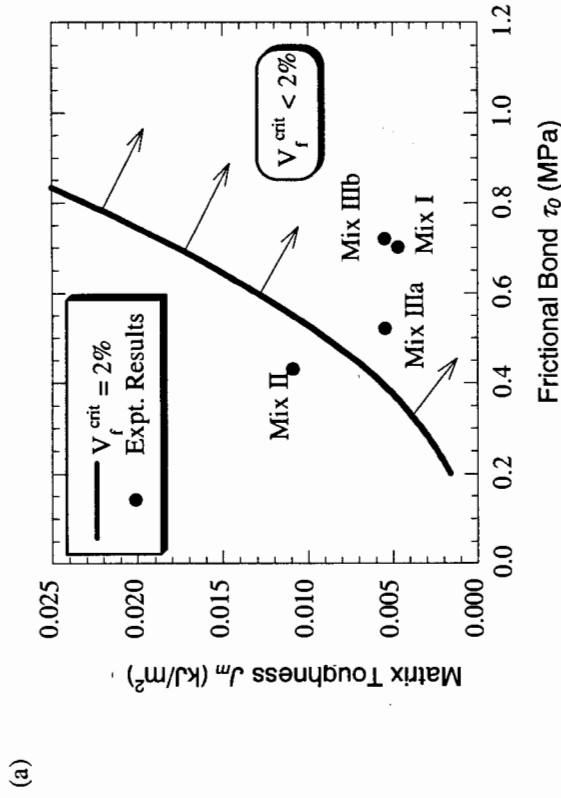


Figure 3: (a) Theoretical boundary between strain-hardening and quasi-brittle behavior using Eqn. (2) and the positions in the ( $J_m$ ,  $\tau_0$ ) space for four composites tested. Shaded region indicates strain-hardening achievable with  $V_f < 2\%$ . (b) Experimentally determined tensile stress-strain curves for the four composites shown in (a).

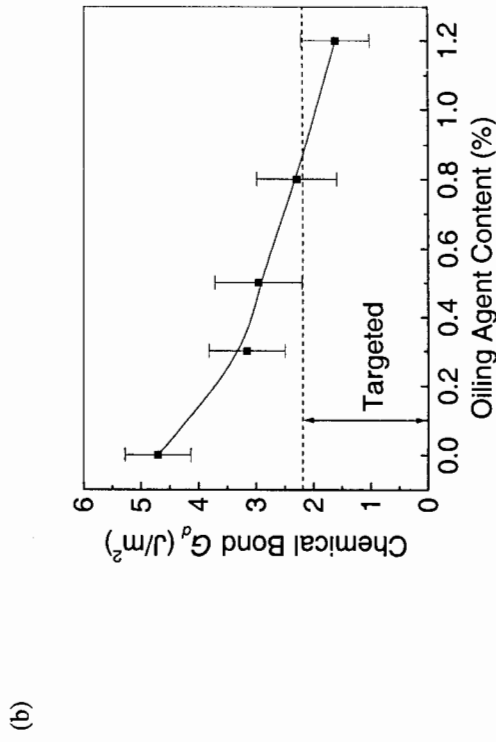
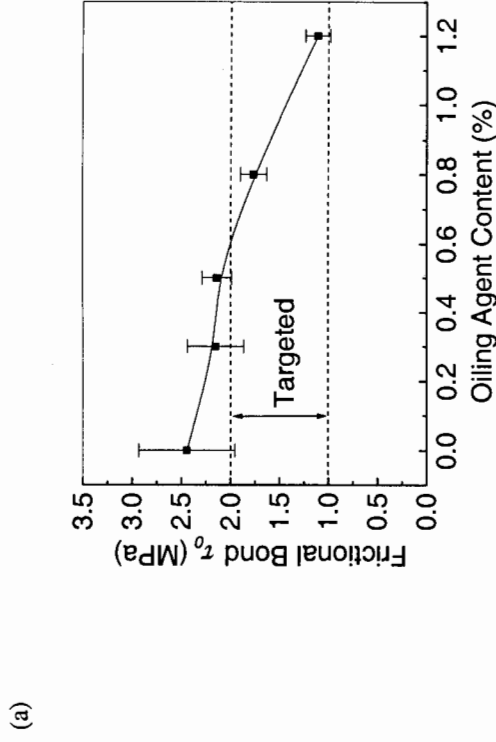


Figure 4: Measured (a)  $\tau_0$  and (b)  $G_d$  as a function of oiling content. Also shown are the target values determined theoretically.

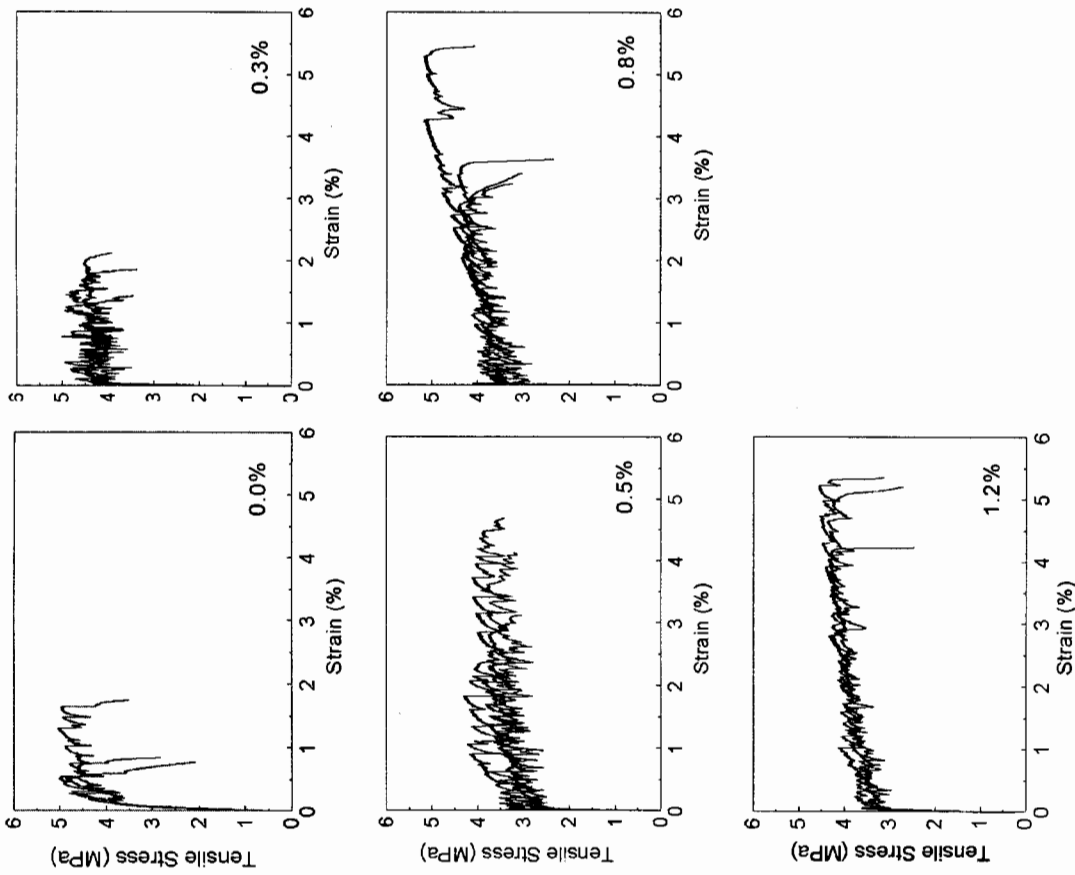
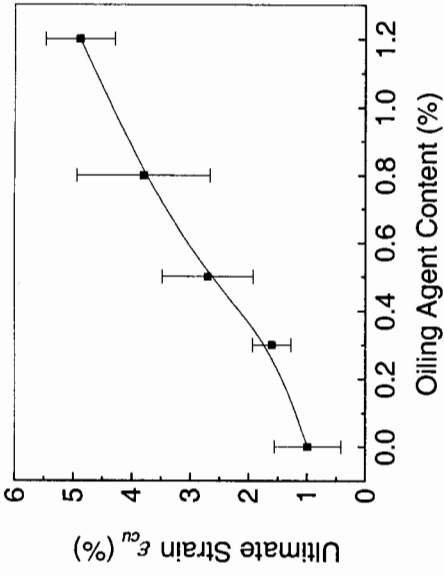


Figure 5: Ductility of the composites as a function of oiling content.

(a)



(b)

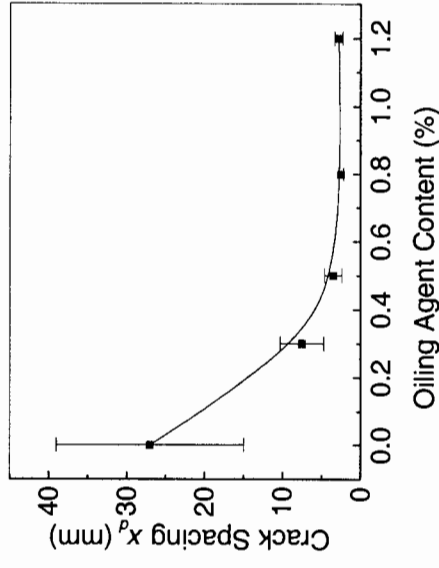
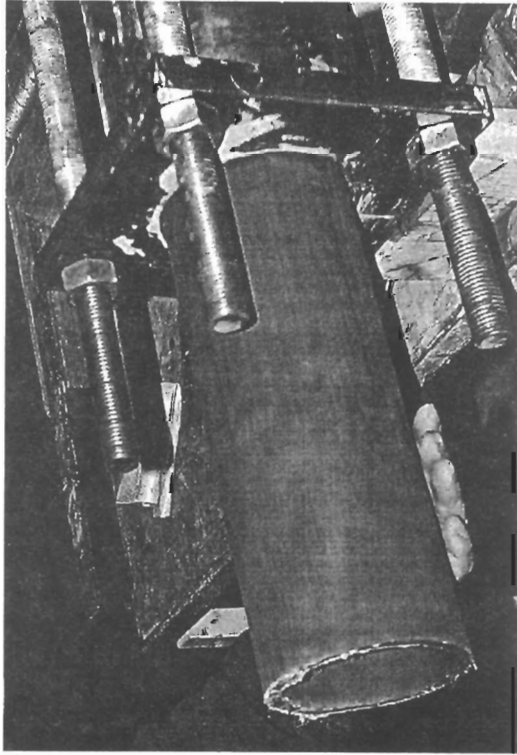


Figure 6: (a) Tensile strain capacity and (b) multiple crack spacing as a function of oiling content.

(a)



(b)



(c)

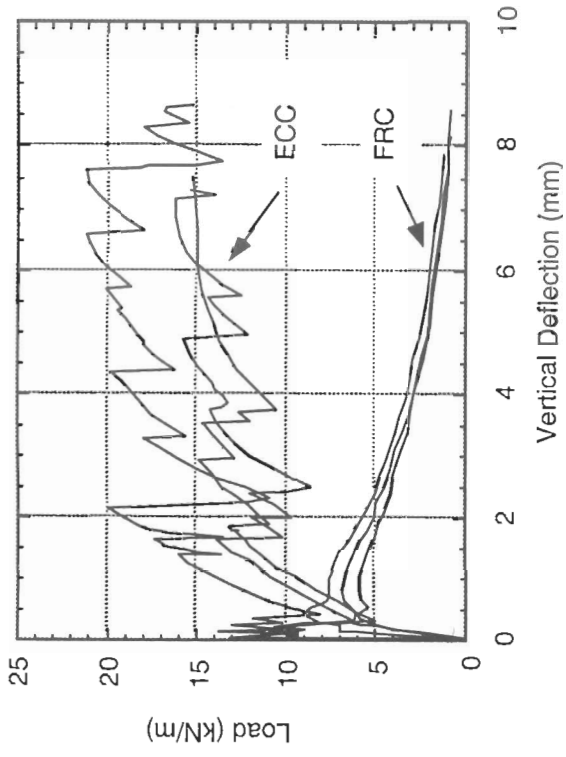
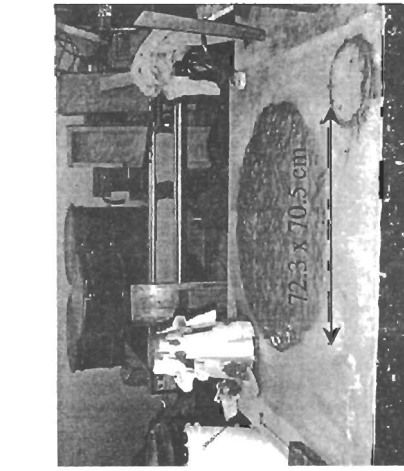
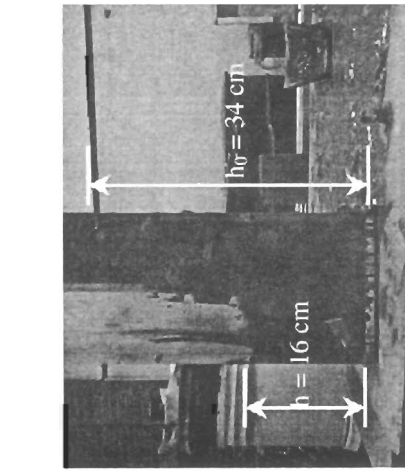


Figure 7: (a) PE-ECC pipe being extruded, (b) Ductile deformation of pipe under ring load, (c) Load-deflection curves for PE-ECC. Also shown for contrast are curves for PP-FRC pipe.

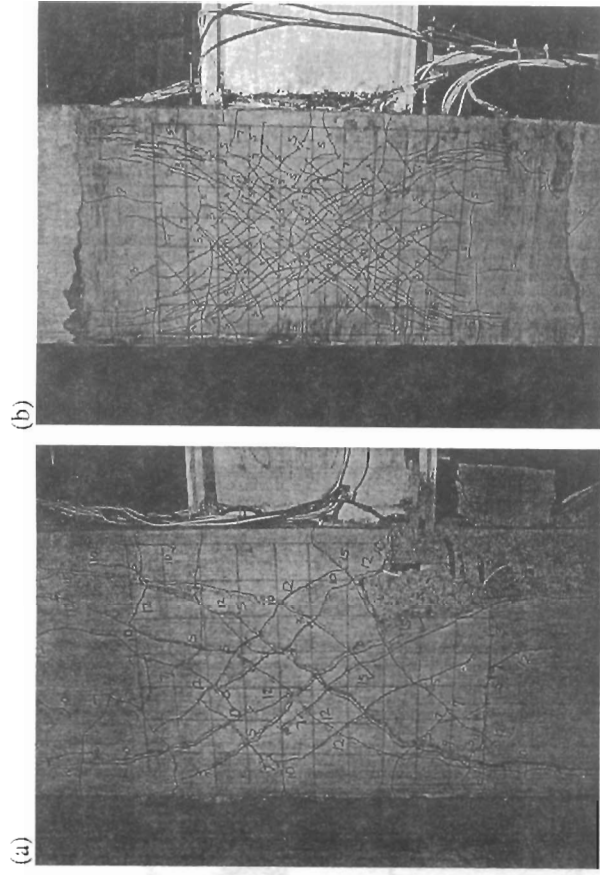


(a)



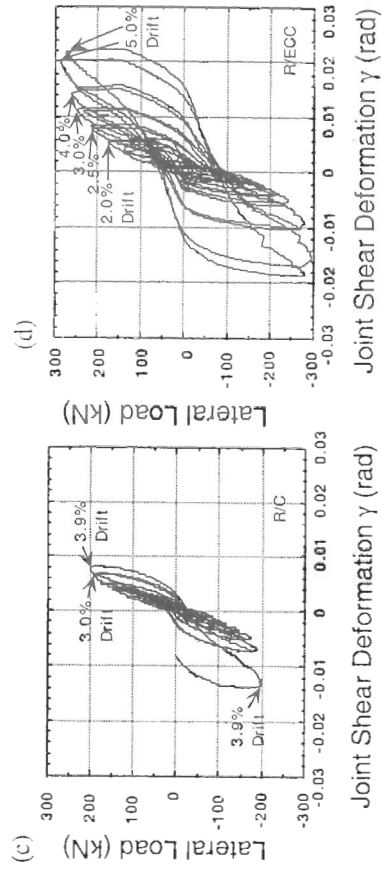
(b)

Figure 8: Result of (a) a deformability test of a self-compacting PVA-ECC ( $\Gamma = 11.7$ ), and (b) a box test of a self-compacting PVA-ECC ( $L = 0.94$ ).



(a)

(b)



(c)

(d)

Figure 9: Damage of joint panel in RCS connection subjected to cyclic loading for (a) standard R/C joint; and (b) R/ECC joint. The corresponding load – joint deformation hysteresis loop for (c) standard R/C joint; and (d) R/ECC joint are also shown.

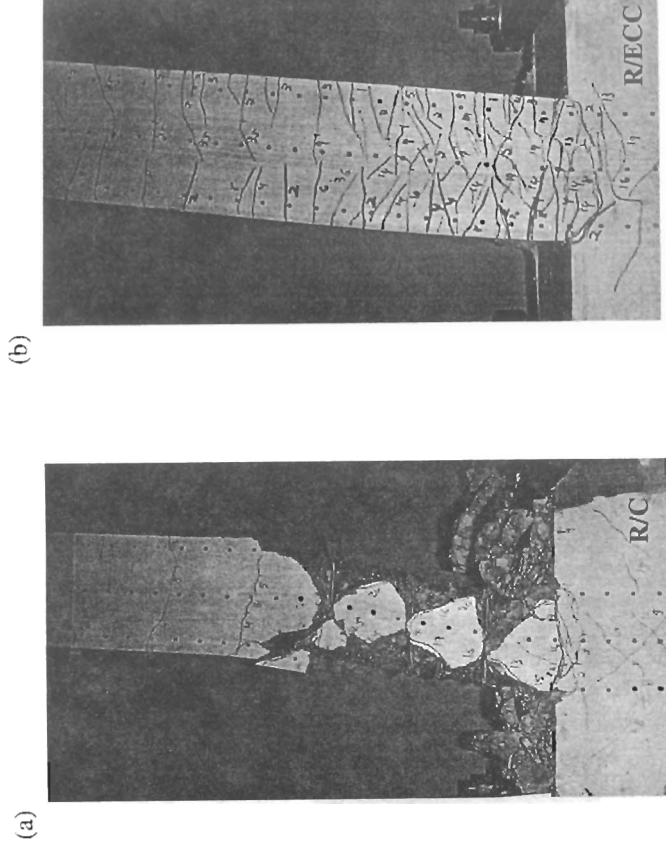


Figure 11: Damage of beam element subjected to flexural cyclic loading for (a) standard R/C beam; and (b) R/ECC beam. The corresponding load – beam deformation hysteresis loops for (c) standard R/C beam; and (d) R/ECC beam are also shown.

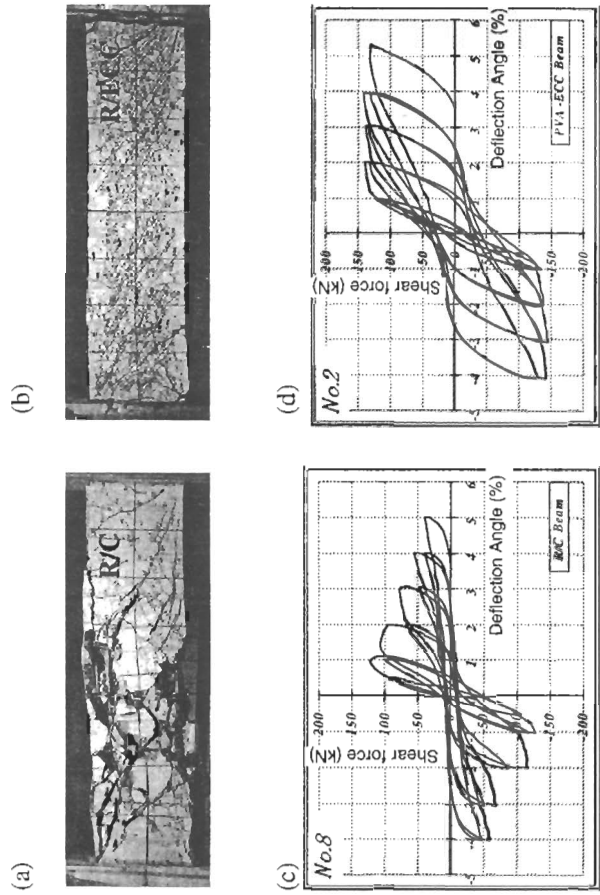


Figure 10: Damage of beam element subjected to shear cyclic loading for (a) standard R/C beam; and (b) R/ECC beam. The corresponding load – beam deformation hysteresis loops for (c) standard R/C beam; and (d) R/ECC beam are also shown.

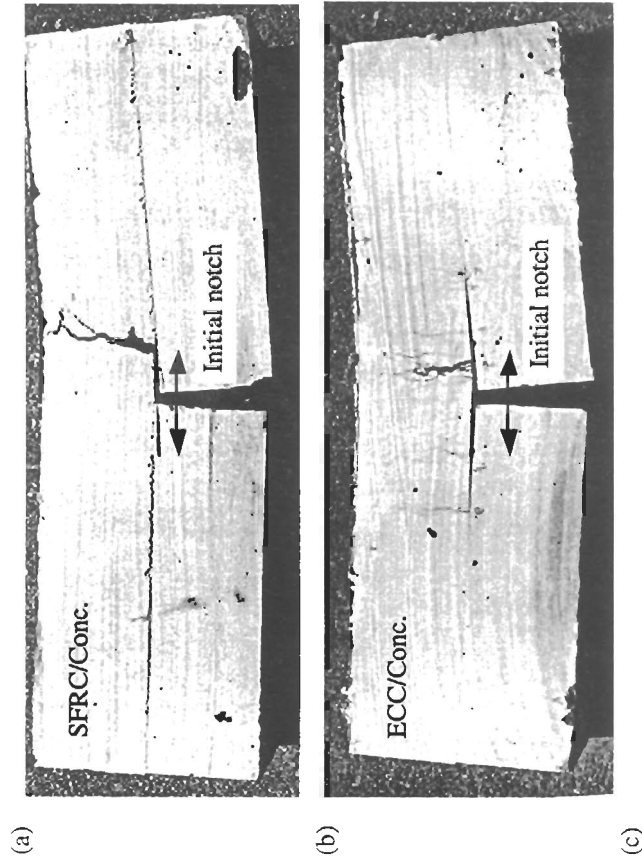


Figure 12: Damage of overlay system subjected to four point bend loading for (a) FRC overlay; and (b) ECC overlay. The corresponding load – deflection curves for standard concrete, FRC, and ECC overlay systems are shown in (c).

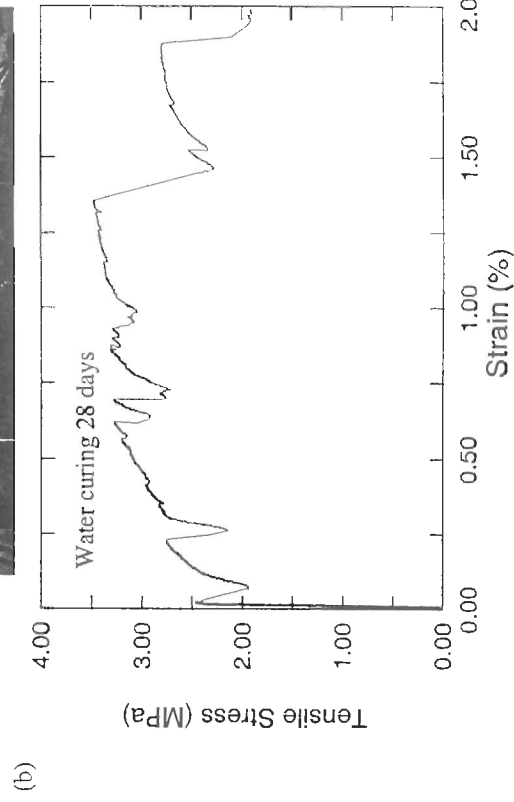
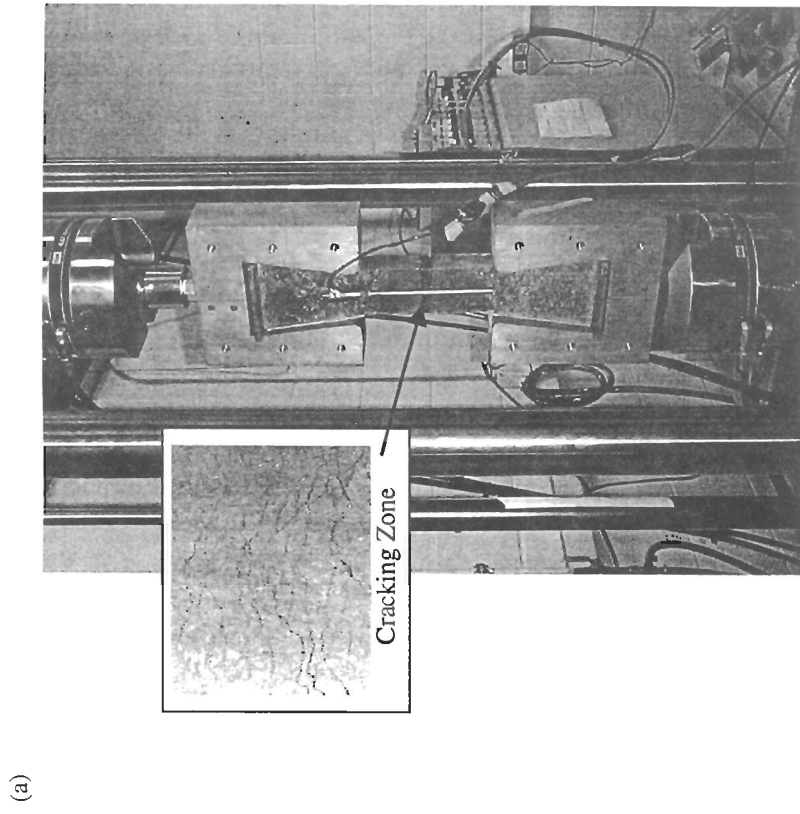


Figure 13: (a) Ductile strip specimen with ECC sandwiched between two standard concrete slabs subjected to simulated restrained shrinkage tensile loading. The corresponding load-deformation curve is shown in (b).

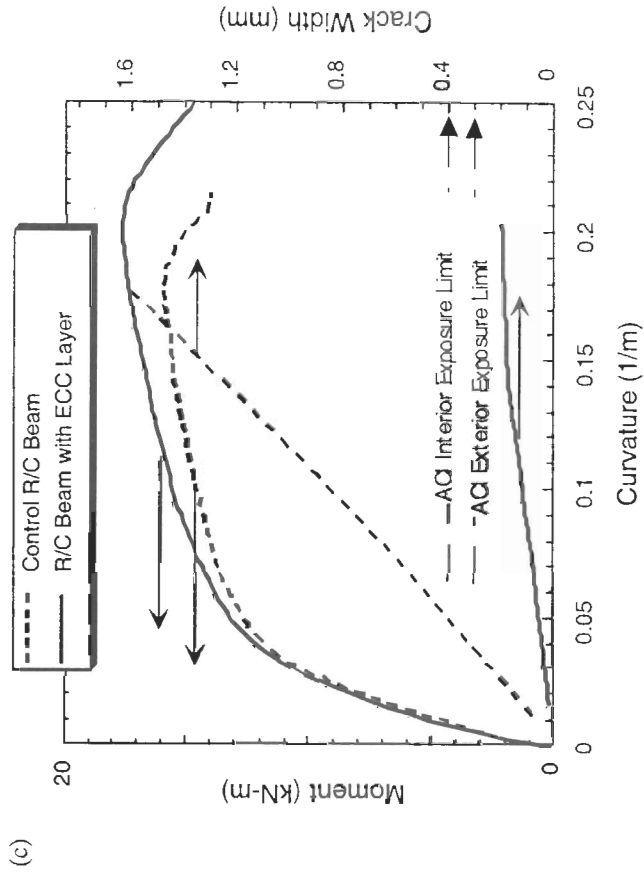
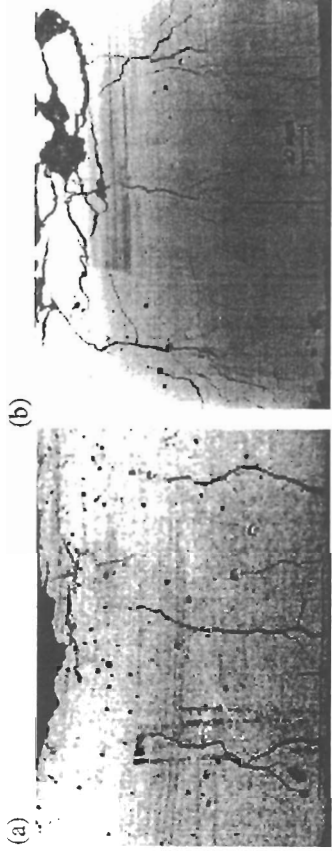


Figure 14: Damage of R/C beam subjected to four point bend loading for (a) standard concrete cover; and (b) ECC cover. The corresponding load – beam deflection curves and crack width in the cover are shown in (c).